A Coordinates and Geometries of Calculated Structures

Given below are the coordinates of main reaction products observed in the $Pt_n^+ + N_2O$ reaction for n=3-6 calculated using Gaussian[1] suite of programs at the def2TZVP[2]/TPSSh[3, 4] level. Also implemented were the GD3-BJ[5] dispersion term, which accounts for weak intramolecular interactions and the quasirelativistic Wood-Boring effective core potential (WB-ECP)[6] that freezes 60 inner electrons and introduces relativistic corrections for Pt atoms.

For n=3-5, N_2O is observed molecularly-bound to the metal cluster via the N atom. For n=6, the cluster reacts with N_2O to generate the Pt_6O^+ product.

Also, given below are the geometries for $2S+1 = 6$ IRC pathway for $Pt_5^+ + N_2O$ reaction outcome.

I. $Pt_3(N_2O)^+$

a) ($2S+1 = 2$)

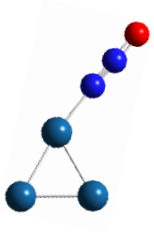

Pt	-0.93779200	-0.63074800	0.00417600
Pt	1.55547200	-0.76759000	-0.00321100
Pt	0.52438600	1.38280400	0.00059700
O	-5.11894800	0.32170800	-0.01540000
N	-3.98427400	0.04334900	-0.00571300
N	-2.89138000	-0.23791600	0.00590000

b) ($2S+1 = 4$)

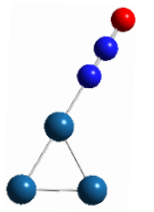

Pt	0.62076600	-1.38245200	0.00000000
Pt	1.53599900	0.87415300	0.00128500
Pt	-0.97916400	0.50092600	-0.00197700
O	-5.26453800	-0.13575100	0.00682800
N	-4.11091500	0.03556000	0.00248400
N	-2.99431300	0.20173700	-0.00258100

Figure S1. a) Lowest energy doublet and b) low-lying (+0.11 eV) quartet structures of molecularly-bound $Pt_3(N_2O)^+$ – the main reaction product observed experimentally.

II. $Pt_4(N_2O)^+$

a) ($2S+1 = 4$)

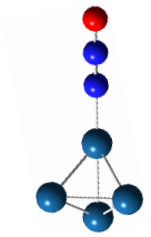

Pt	0.53137100	0.88276400	1.27656800
Pt	0.53138600	0.88240500	-1.27681100
Pt	1.32125100	-1.17013300	0.00017800
Pt	-1.16655100	-0.60650600	0.00006000
O	-5.39729200	0.26259400	-0.00001100
N	-4.25188700	0.02750600	0.00002900
N	-3.14573200	-0.19979900	0.00004000

b) ($2S+1 = 2$)

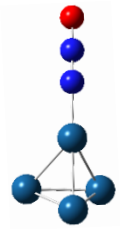

Pt	0.57927000	0.00748300	1.54431000
Pt	0.46313600	-1.47263300	-0.55045900
Pt	-1.15946900	0.54783000	-0.34298700
Pt	1.32243000	0.92713800	-0.67647700
O	-5.34891700	-0.23509200	0.23938300
N	-4.20887400	-0.02316700	0.08209000
N	-3.10930400	0.18245500	-0.07027600

Figure S2. a) Lowest energy quartet and b) low-lying (+0.24 eV) doublet structures of molecularly-bound $Pt_4(N_2O)^+$ – the main reaction product observed experimentally.

III. $Pt_5(N_2O)^+$

a) ($2S+1 = 4$)

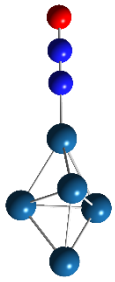

Pt	-0.29114500	-0.12343700	-1.47921800
Pt	-0.29185100	1.34283600	0.63276900
Pt	-2.42459900	-0.00025200	-0.00040500
Pt	1.88059800	0.00035000	0.00043100
Pt	-0.29153900	-1.21934800	0.84659600
O	6.13486100	-0.00050500	-0.00097200
N	4.96295300	-0.00095900	-0.00073000
N	3.83231700	-0.00012000	-0.00009600

b) ($2S+1 = 6$)

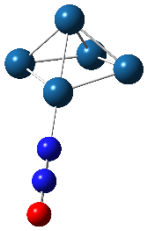

Pt	0.13734500	1.94241500	-0.16681200
Pt	0.14090600	-1.94234400	-0.16739000
Pt	1.47113100	0.00138600	-1.17385500
Pt	-1.45239600	-0.00147500	0.39621900
Pt	0.94607500	0.00056500	1.33715500
O	-5.42461200	-0.00097800	-1.22729700
N	-4.34555300	-0.00185900	-0.77419500
N	-3.30613400	-0.00310800	-0.33384300

Figure S3. a) Lowest energy quartet and b) low-lying (+0.20 eV) sextet structures of molecularly-bound $Pt_5(N_2O)^+$ – the main reaction product observed experimentally.

IV. $Pt_6(O)^+$

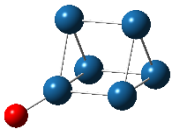

Pt	1.54595500	1.06468100	0.00009700
Pt	-1.48627700	-0.42631500	-1.27330500
Pt	-0.85298100	1.69697200	0.00140500
Pt	-1.48394600	-0.42811900	1.27461100
Pt	0.98840800	-1.06065300	1.27764000
Pt	0.98633100	-1.05845200	-1.28051400
O	2.94945900	2.06589500	0.00065700

Figure S4. Lowest energy (2*S* +1 = 6) calculated Pt_6O^+ structure – the dominant reaction product observed following the Pt_6^++ N_2O reaction.

V. IRC for the Pt_5^+ + N_2O Reaction Showing Sextet Structures

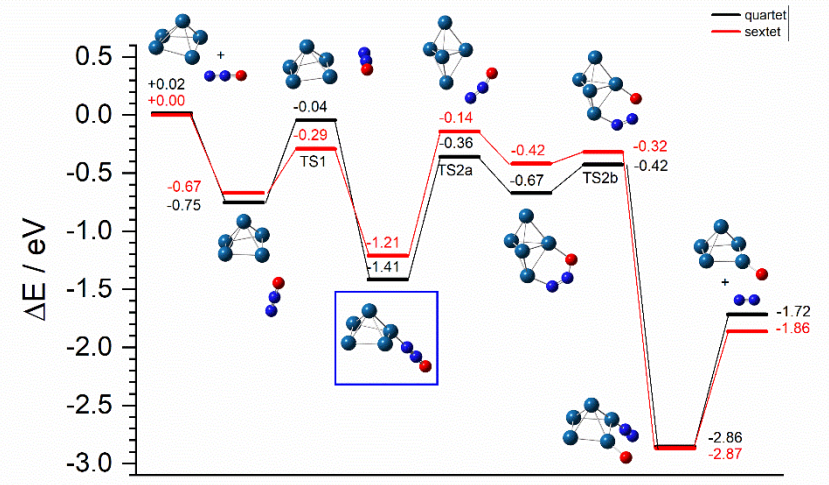

Figure S5. IRC pathway for the Pt_5^++ N_2O reaction; as Figure 3b) in the main manuscript but with calculated sextet structures shown.

B. N_2O Binding Energies and Bond Lengths

Given below are the calculated binding energies of N_2O to Pt_n^+ (n=1-5) along with Pt-N, N=N, and N=O bond lengths for the lowest energy molecularly-bound structures.

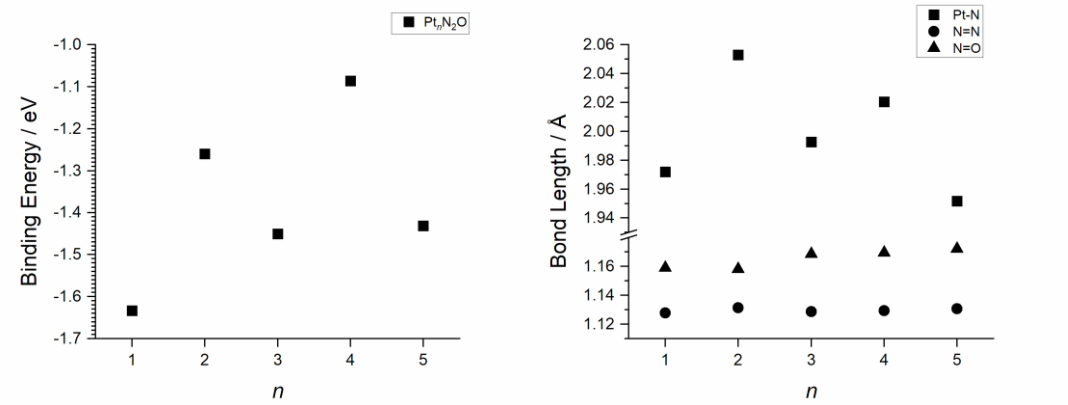

Figure S6. Calculated N_2O binding energies and bond lengths of lowest-energy N-bound $Pt_nN_2O^+$ structures.

References

1. Gaussian 16 Revision C.01, M. J. Frisch, G. W. Trucks, H. B. Schlegel, G. E. Scuseria, M. A. Robb, J. R. Cheeseman, G. Scalmani, V. Barone, G. A. Petersson, H. Nakatsuji, X. Li, M. Caricato, A. V. Marenich, J. Bloino, B. G. Janesko, R. Gomperts, B. Mennucci, H. P. Hratchian, J. V. Ortiz, A. F. Izmaylov, J. L. Sonnenberg, Williams, F. Ding, F. Lipparini, F. Egidi, J. Goings, B. Peng, A. Petrone, T. Henderson, D. Ranasinghe, V. G. Zakrzewski, J. Gao, N. Rega, G. Zheng, W. Liang, M. Hada, M. Ehara, K. Toyota, R. Fukuda, J. Hasegawa, M. Ishida, T. Nakajima, Y. Honda, O. Kitao, H. Nakai, T. Vreven, K. Throssell, J. A. Montgomery Jr., J. E. Peralta, F. Ogliaro, M. J. Bearpark, J. J. Heyd, E. N. Brothers, K. N. Kudin, V. N. Staroverov, T. A. Keith, R. Kobayashi, J. Normand, K. Raghavachari, A. P. Rendell, J. C. Burant, S. S. Iyengar, J. Tomasi, M. Cossi, J. M. Millam, M. Klene, C. Adamo, R. Cammi, J. W. Ochterski, R. L. Martin, K. Morokuma, O. Farkas, J. B. Foresman and D. J. Fox, Gaussian, Inc., Wallingford CT, 2016.
2. F. Weigend and R. Ahlrichs, *Phys. Chem. Chem. Phys.*, 2005, **7**, 3297-3305.
3. V. N. Staroverov, G. E. Scuseria, J. Tao and J. P. Perdew, *J. Chem. Phys.*, 2003, **119**, 12129-12137.
4. J. Tao, J. P. Perdew, V. N. Staroverov and G. E. Scuseria, *Phys. Rev. Lett.*, 2003, **91**, 146401.
5. S. Grimme, S. Ehrlich and L. Goerigk, *J. Comput. Chem.*, 2011, **32**, 1456-1465.
6. D. Andrae, U. Häußermann, M. Dolg, H. Stoll and H. Preuß, *Theor. Chim. Acta*, 1990, **77**, 123-141.